Unknown Input Observer Based Approach for Distributed Tube-Based Model Predictive Control of Heterogeneous Vehicle Platoons

Qianyue Luo, Anh-Tu Nguyen, *Member, IEEE*, James Fleming, and Hui Zhang, *Senior Member, IEEE*

***Abstract*—This paper addresses the control problem of heterogeneous vehicle platoons subject to disturbances and modeling errors. The objective is to guarantee spatial-geometry constraints of vehicles in a platoon. We deal with the case where a predecessor-leader following (PLF) communication topology is used and heterogeneous vehicle dynamics is subject to disturbances. To estimate the lumped disturbance, the technique of unknown input proportional multiple-integral (PMI) observer is employed such that both the state and the disturbance are simultaneously estimated. Moreover, tube-based model predictive control (TMPC) is used and the corresponding control law is composed of a feed-forward term, a feedback term, and a disturbance compensation term. The gains in the integrated control strategy are optimized by utilizing the particle swarm optimization (PSO) algorithm with an $\mathscr{H}_\infty$ performance index of an augmented error system. It is proved that the deviations between the actual system and the nominal system are bounded in a robustly positively invariant (RPI) set, that is, the main objective is guaranteed. With the proposed control strategy, simulations and comparisons are carried out. We can see that the control performance of the proposed strategy is significantly improved while the computational time is reduced compared with existing methods.**

***Index Terms*—Integrated controller, proportional multiple-integral (PMI) observer, tube -based model predictive control (TMPC), vehicle platoon.**

I. Introduction

INTELLIGENT transportation and multi-vehicle coordination are becoming a promising area both from industry and academic research. Among the applications, vehicle platooning has great advantages in terms of efficiency, safety, energy consumption, and environmental protection [1]–[5]. The technique of vehicle platooning is based on the vehicle-to-vehicle (V2V) communication technology. The main function is to make multiple vehicles driving on the same lane with a close range and same velocity [6], [7].

Generally, vehicle platoon control is more challenging than the traditional vehicle dynamics control. The challenges and differences arise from the following aspects.

1) The models for controller design are different. In order to reduce the computational burden, a simplified model is used for platoon controller design. In the literature, there are second-order models with speed and displacement as two system states [8], [9], third-order models with one more acceleration state [10]–[12], and three-state models with lateral dynamics [13], [14].
2) Information from other vehicles is necessary for platoon control in which each vehicle communicates with other vehicles according to the communication topology. The selection and the design of communication topology have a crucial impact on platoon stability [15], [16].
3) The design objectives are different. The objective of platoon control is not only to ensure the stability of individual vehicle but also to ensure the platoon stability. The overall position error of the platoon should not be amplified as the number of vehicles increased, which is also known as string stability [17]–[19]. Due to the energy-saving characteristics of vehicle platoons, the energy consumption may be considered as an additional control objective [8].
4) More constraints should be considered for platoon control. Besides original constraints of individual vehicle control, the constraints of the platoon control should include the position, speed and acceleration constraints between the adjacent vehicles.

In addition to different platoon models, different control strategies have been applied for platoon control. The authors in [7] adopted a frequency-domain design method for a cooperative adaptive cruise control. Sliding mode control strategies were proposed in [20], [21]. An $\mathscr{H}_\infty$ control method was employed in [22], [23]. Moreover, distributed model predictive control (DMPC) has been applied in various contexts [16], [24], [25]. From the application perspective, the platoon control is a multi-objective optimization problem under multiple physical

Manuscript received April 17, 2020; revised November 29, 2020 and February 3, 2021; accepted March 2, 2021. Date of publication March 9, 2021; date of current version May 5, 2021. This work was supported in part by the National Natural Science Foundation of China Under Grant U1864201. The review of this article was coordinated by Prof. Yaser P. Fallah. *(Corresponding author: Hui Zhang.)*

Qianyue Luo is with the School of Transportation Science and Engineering, Beihang University, Beijing 100091, China (e-mail: luoqy1996@gmail.com).

Anh-Tu Nguyen is with the Laboratory LAMIH-CNRS, UMR 8201, Université Polytechni que Hauts-De-France, Valenciennes, Hauts-de-France 59300, France, and also with the INSA Hauts-De-France, 59300 Valenciennes, France (e-mail: nguyen.trananhtu@gmail.com).

James Fleming is with the Wolfson School of Mechanical, Electrical and Manufacturing Engineering, Loughborough University, Loughborough LE11 3TU, U.K. (e-mail: J.Fleming@lboro.ac.uk).

Hui Zhang is with the School of Transportation Science and Engineering, Beihang University, Beijing 100091, China and also with the Ningbo Institute of Technology (NIT), Beihang University, Ningbo 315323, China (e-mail: huizhang285@gmail.com).

Digital Object Identifier 10.1109/TVT.2021.3064680

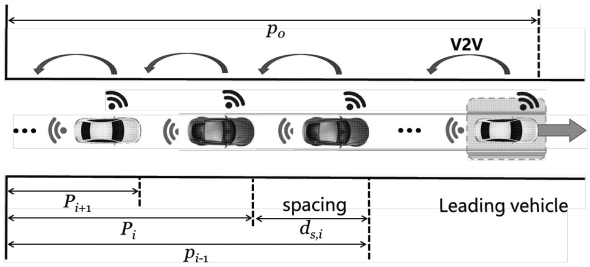

Fig. 1. A scenario and structure of vehicle platoons.

constraints and external disturbances. Though there are considerable existing control strategies for this control problem, few results are obtained by considering *simultaneously* the physical constraints and external disturbances.

Model predictive control (MPC) has been known as powerful tool to deal with system constraints. However, when the system is subject to persistent disturbances, the constraints may not be satisfied if the disturbances are not explicitly considered in MPC design. When the system is subject to persistent disturbances, Mayne and Langson proposed tube-based model predictive control (TMPC) to solve the optimization problem [26]–[28]. Then, it was applied to applications such as vehicle control in [29], [30] by adding feedback terms to make the error caused by disturbance converging to an invariant set [31]–[33]. In this work, we employ the tube-based idea to design a robust controller for heterogeneous vehicle platoons subject to both modeling uncertainties and external disturbances. The main contributions of this paper are three-fold: 1) A proportional multiple-integral (PMI) observer is designed to estimate both the system state and the lumped disturbance for DMPC purposes such that the number of physical sensors can be reduced; 2) A compensation term is integrated in the control law to compensate the effects of disturbances such that the conservativeness of the TMPC algorithm is reduced and the robustness performance is improved; 3) $\mathscr{H}_\infty$ control performance and particle swarm optimization (PSO) algorithm are adopted to optimally tune both the observer and controller gains, allowing to minimizing the disturbance impacts.

Notation: $\mathbb{R}$ and $\mathbb{N}$ stand for the set of real numbers and positive integers, respectively. For $p \in \mathbb{N}$ and a vector $x \in \mathbb{R}^n$, the p-norm of x is given as $\|x\|_p = (\sum |x_i|^p)^{1/p}$, while $\|x\|_\infty = \max |x_i|$; for a vector $x \in \mathbb{R}^n$ and a positive semi-definite matrix $Q \in \mathbb{R}^{n\times n}$, $\|x\|_Q = (x^T Q x)^{1/2}$ denotes the weighted Euclidean norm of x. The Minkowski sum of sets $\mathbb{P}, \mathbb{Q}$ is $\mathbb{P} \oplus \mathbb{Q} = \{x + y | x \in \mathbb{P}, y \in \mathbb{Q}\}$; the Pontryagin difference of sets $\mathbb{P}, \mathbb{Q}$ is $\mathbb{P} \ominus \mathbb{Q} = \{x | x + y \in \mathbb{P}, y \in \mathbb{Q}\}$. $\bar{x}$ denotes the nominal value of x, and $\hat{x}$ denotes the observed value of x. The rest of notations will be provided in the paper.

II. Modeling and Preliminary

Vehicle platoons are composed of one leading vehicle (numbered with 0) and N following vehicles (numbered from 1 to N) in the same lane, see Fig. 1. The vehicles in a platoon can be heterogeneous or homogeneous. Hereafter, we discuss the three main elements of a model-based control scheme for vehicle platooning: longitudinal dynamics of each vehicle, communication connection topology between vehicles, and goals of vehicle platooning.

A. Vehicle Longitudinal Dynamics

We consider the longitudinal control of vehicles subject to multiple resistances [16], including wind resistance, rolling resistance, and slope resistance. The longitudinal dynamics of ith vehicle is described as

$$\begin{aligned} p_i(k+1) &= p_i(k) + v_i(k)\Delta t \\ v_i(k+1) &= v_i(k) + \left(\frac{\eta_i}{m_i r_i} T_i(k) - a_{fi}(v_i(k))\right)\Delta t \\ T_i(k+1) &= T_i(k) + (u_i(k) - T_i(k))\frac{\Delta t}{\tau_i} + w_i(k) \end{aligned} \tag{1}$$

where the vehicle $p_i(k)$ is the vehicle position, $v_i(k)$ is the vehicle velocity, $T_i(k)$ is the integrated driving/braking torque, the control input $u_i(k)$ represents the desired driving/braking torque, Δt is the discrete time interval, η_i is the transmission efficiency, m_i is the vehicle mass, r_i is the tire radius, τ_i is the inertial lag of longitudinal dynamics, C_{Ai} is the coefficient of aerodynamic drag, g is the gravity constant, f_i is the coefficient of rolling resistance, and θ_i is the slope angle. The disturbance $w_i(k)$ represents the lumped disturbance that contains external disturbances and the modeling errors [34], [35]. Assume that the disturbance is amplitude-bounded, *i.e.*, $w_i(k) \in \mathbb{W}_i$, where $\mathbb{W}_i$ is a compact interval containing the origin in its interior. The nonlinearity $a_{fi}(v_i(k))$ is given by

$$a_{fi}(v_i(k)) = C_{Ai} v_i^2(k) + g f_i \cos(\theta_i) + g \sin(\theta_i).$$

We denote the state vector $x_i(k) = [p_i(k) \;\; v_i(k) \;\; T_i(k)]^\top$, and the system output $y_i(k) = p_i(k)$. Then, model (1) can be reformulated in the state-space form

$$\begin{aligned} x_i(k+1) &= A_i x_i(k) + g_i(x_i(k)) + B_i u_i(k) + G_i + H w_i(k) \\ y_i(k) &= C x_i(k) \end{aligned} \tag{2}$$

where

$$A_i = \begin{bmatrix} 1 & \Delta t & 0 \\ 0 & 1 & \frac{\eta_i \Delta t}{m_i r_i} \\ 0 & 0 & 1 - \frac{\Delta t}{\tau_i} \end{bmatrix}, \quad B_i = \begin{bmatrix} 0 \\ 0 \\ \frac{\Delta t}{\tau_i} \end{bmatrix},$$

$$G_i = \begin{bmatrix} 0 \\ -g f_i \cos(\theta) - g \sin(\theta) \\ 0 \end{bmatrix}, \quad H = \begin{bmatrix} 0 \\ 0 \\ 1 \end{bmatrix},$$

$$g_i(x_i(k)) = \begin{bmatrix} 0 \\ -C_{Ai} v_i^2(k) \\ 0 \end{bmatrix}, \quad C = \begin{bmatrix} 1 \\ 0 \\ 0 \end{bmatrix}^\top.$$

The system is subject to both state and control constraints as

$$u_i \in \mathbb{U}_i, \quad x_i \in \mathbb{X}_i,$$

where $\mathbb{U}_i \in \mathbb{R}^1$ is a compact set, $\mathbb{X}_i \in \mathbb{R}^{3\times 1}$ is a closed set, and each set contains the origin in its interior.

Without taking into account the bounded disturbance $w_i(k)$, the *nominal* longitudinal dynamics of ith vehicle associated with

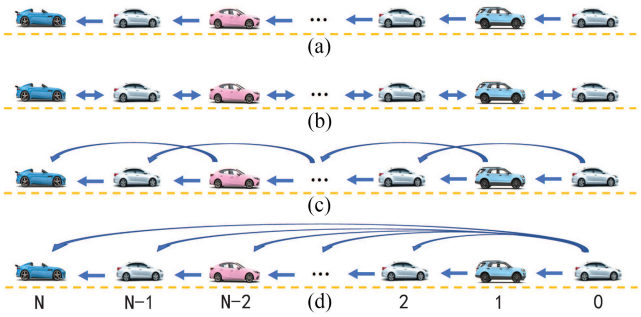

Fig. 2. Common communication topology for vehicle platoons. (a) predecessor-following (PF), (b) bidirectional following (BF), (c) two-predecessor following (TPF), (d) predecessor-leader following (PLF).

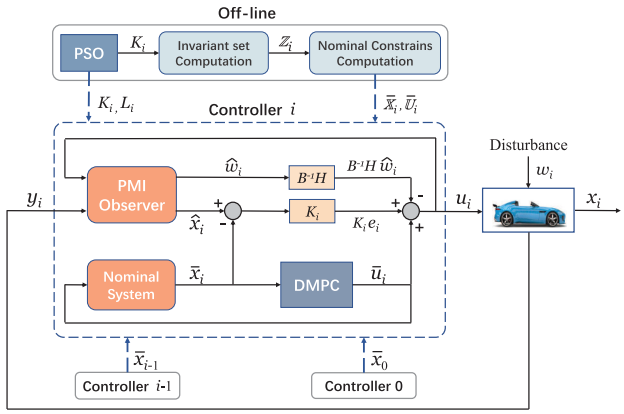

Fig. 3. Structure of the proposed integrated control scheme.

system (2) is given by

$$\bar{x}_i(k+1) = A_i\bar{x}_i(k) + g_i(\bar{x}_i(k)) + B_i\bar{u}_i(k) + G_i$$
$$\bar{y}_i(k) = C\bar{x}_i(k). \tag{3}$$

Note that for any time-varying variable $s(k)$ of the vehicle system (2), $\bar{s}(k)$ denotes the corresponding variable of its nominal model (3).

B. Communication Structure of Vehicle Platoons

With the development of V2V technology, a rapid local vehicular communication can be realized. Individual vehicles are connected via communication to form a vehicle platoon structure. Several communication topologies are available in the literature [16], which are illustrated in Fig. 2.

Here, the predecessor-leader following (PLF) communication topology is adopted, which has been widely used and discussed [36], [37]. In a PLF topology, each vehicle can receive the information transmitted from the predecessor-vehicle and the leader-vehicle. It has been shown that this communication structure can help the platoon state converge to a stable state more securely by directly using the information from the leader-vehicle [12]. The information includes its planned trajectory (or vehicle states) and the desired inter-vehicle spacing.

C. Platooning Control Objectives

The primary goal of platooning is to maintain a desired safe spacing between vehicles and to drive each vehicle at the same speed on the same lane with the leading vehicle under the effects of external disturbances and modeling errors. For system (2) with the lumped disturbance $w_i(k) \in \mathbb{W}_i$, this goal can be mathematically represented as

$$\lim_{k\to\infty} \begin{bmatrix} p_i(k) - p_0(k) + i\cdot d_0 \\ v_i(k) - v_0(k) \\ a_i(x_i(k)) \end{bmatrix} \in \sigma_i,\ i \in \mathbb{N}, \tag{4}$$

where d_0 is the desired space between adjacent vehicles, $v_0(k)$ is the desired speed and $a_i(x_i(k)) = \frac{\eta_i}{m_i r_i}T_i(k) - a_{fi}(v_i(k))$ is the acceleration of ith vehicle, σ_i is an invariant set and its size depends on the system disturbance and controller parameters (see Section III).

To evaluate the control performance, we consider two following variables: i) the spacing $d_{si}(k)$ between the adjacent vehicles, ii) the platoon deviation $\Delta d_{pi}(k)$, which are respectively defined as

$$d_{si}(k) = p_{i-1}(k) - p_i(k),\ \Delta d_{pi}(k) = p_0(k) - p_i(k) - id_0,$$

for $i \in \mathbb{N}$.

III. Control Problem Formulation

To achieve the control goal specified in (4) for system (2), we propose an integrated control scheme composed of three components: feedback control, disturbance-compensation control and feedforward control, see Fig. 3. Then, the new integrated control law of ith vehicle is of the form

$$u_i(k) = \bar{u}_i(k) + K_i(\hat{x}_i(k) - \bar{x}_i(k)) - B_i^{\dagger}H\hat{w}_i(k), \tag{5}$$

where $\bar{u}_i$ denotes the feedforward control, K_i is the feedback gain to be designed, $B_i^{\dagger} = (B_i^{\top}B_i)^{-1}B_i^{\top}$ is the pseudo-inverse of the full-collum rank matrix B_i, and $\hat{x}_i$ and $\hat{w}_i$ are respectively the estimates of x_i and w_i. The design procedure of the integrated control law (5) is described as follows.

A. Design of Feedback Control and Disturbance-Compensation Control

This section presents the design of an PMI observer to estimate both the state x_i and the disturbance w_i for the vehicle system (2). The proposed PMI observer can achieve a high-precision estimation performance for systems with high order time-varying disturbances. In particular, it can provide an asymptotic estimation performance for polynomial disturbances [38]. This not only reduces the number of physical vehicle sensors used for feedback control but also allows to construct a disturbance-compensation action in the integrated control law (5).

1) Proportional Multiple Integral Observer: For state and disturbance estimation, we make use of the following third-order PMI observer:

$$\hat{x}_i(k+1) = A_i\hat{x}_i(k) + g_i(\hat{x}_i(k)) + B_iu_i(k) + G_i + H\hat{w}_i(k) + L_{Pi}(y_i(k) - \hat{y}_i(k))$$
$$\hat{w}_i(k+1) = \hat{w}_i(k) + \hat{w}_{1i}(k)\Delta t + L_{I1i}(y_i(k) - \hat{y}_i(k))$$

$$\begin{aligned}\hat{w}_{1i}(k+1) &= \hat{w}_{1i}(k) + \hat{w}_{2i}(k)\Delta t + L_{I2i}(y_i(k) - \hat{y}_i(k))\\ \hat{w}_{2i}(k+1) &= \hat{w}_{2i}(k) + L_{I3i}(y_i(k) - \hat{y}_i(k))\\ \hat{y}_i(k) &= C\hat{x}_i(k)\end{aligned} \tag{6}$$

where L_{Pi}, L_{I1i}, L_{I2i} and L_{I3i} are the observer gains to be determined.

We assume that the dynamics of the time-varying lumped disturbance $w_i(k)$ is given as follows:

$$\begin{aligned}w_i(k+1) &= w_i(k) + w_{1i}(k)\Delta t\\ w_{1i}(k+1) &= w_{1i}(k) + w_{2i}(k)\Delta t\\ w_{2i}(k+1) &= w_{2i}(k) + w_{ei}(k)\end{aligned} \tag{7}$$

with $w_{ei}(k) \in \mathbb{W}_{ei}$. Then, the estimation errors are defined as

$$e_{\hat{x}_i}(k) = x_i(k) - \hat{x}_i(k), \qquad e_{w_i}(k) = w_i(k) - \hat{w}_i(k),$$

$$e_{w_{1i}}(k) = w_{1i}(k) - \hat{w}_{1i}(k), \quad e_{w_{2i}}(k) = w_{2i}(k) - \hat{w}_{2i}(k).$$

Therefore, the dynamics of the estimation errors can be obtained from (2), (6) and (7) as

$$\begin{aligned}e_{\hat{x}_i}(k+1) &= (A_i - L_{Pi}C)e_{\hat{x}_i}(k) + He_{w_i}(k) + \delta_{\hat{g}_i}(k)\\ e_{w_i}(k+1) &= e_{w_i}(k) + e_{w_{1i}}(k)\Delta t - L_{I1i}Ce_{\hat{x}_i}(k)\\ e_{w_{1i}}(k+1) &= e_{w_{1i}}(k) + e_{w_{2i}}(k)\Delta t - L_{I2i}Ce_{\hat{x}_i}(k)\\ e_{w_{2i}}(k+1) &= e_{w_{2i}}(k) - L_{I3i}Ce_{\hat{x}_i}(k) + w_{ei}(k)\end{aligned} \tag{8}$$

where $\delta_{\hat{g}_i}(k) = g_i(x_i(k)) - g_i(\hat{x}_i(k))$.

2) Analysis of Error Dynamics: Let $e_{x_i}(k) = x_i(k) - \bar{x}_i(k)$ be the state error between the vehicle system (2) and its nominal model (3), whose dynamics is given by

$$\begin{aligned}e_{x_i}(k+1) = (A_i + B_iK_i)e_{x_i}(k) - B_iK_ie_{\hat{x}_i}(k)\\ + He_{w_i}(k) + \delta_{\bar{g}_i}(k),\end{aligned} \tag{9}$$

where $\delta_{\bar{g}_i}(k) = g_i(x_i(k)) - g_i(\bar{x}_i(k))$. Let us define the augmented error state vector as

$$e_i(k) = \begin{bmatrix}e_{x_i}(k) & e_{\hat{x}_i}(k) & e_{w_i}(k) & e_{w_{1i}}(k) & e_{w_{2i}}(k)\end{bmatrix}^\top.$$

It follows from (8) and (9) that

$$e_i(k+1) = A_{ei}e_i(k) + e_{g_i}(k) + B_{ei}w_{ei}(k), \tag{10}$$

where

$$A_{ei} = \begin{bmatrix}A_i + B_iK_i & -B_iK_i & H & 0 & 0\\ 0 & A_i - L_{Pi}C & H & 0 & 0\\ 0 & -L_{I1i}C & 1 & \Delta t & 0\\ 0 & -L_{I2i}C & 0 & 1 & \Delta t\\ 0 & -L_{I3i}C & 0 & 0 & 1\end{bmatrix},$$

$$B_{ei} = \begin{bmatrix}0 & 0 & 0 & 0 & 0 & 0 & 0 & 0 & 1\end{bmatrix}^\top,$$

$$e_{g_i}(k) = \begin{bmatrix}\delta_{\bar{g}_i}(k)^\top & \delta_{\hat{g}_i}(k)^\top & 0 & 0 & 0\end{bmatrix}^\top.$$

Exploiting the Lipschitz property of the nonlinear function $g_i(x)$ over the state set $\mathbb{X}_i$, it follows that [30]

$$\|e_{g_i}\|_\infty \le L_i(\mathbb{X}_i) \max_{e_{vi}\in\mathbb{V}_i} \|e_{vi}\|_2, \tag{11}$$

where $L_i(\mathbb{X}_i)$ is the Lipschitz constant of $g_i(\cdot)$ over $\mathbb{X}_i$, $e_{vi} = \begin{bmatrix}0 & v_i - \bar{v}_i & 0 & 0 & v_i - \hat{v}_i & 0 & 0 & 0 & 0\end{bmatrix}^\top$, $\mathbb{V}_i$ is a subset of $\mathbb{X}_i$ to bound the e_{vi}.

Expression (11) allows defining the following box $\mathbb{B}_g(\mathbb{V}_i)$ to bound the nonlinear term $e_{g_i}(\cdot)$ in system (10):

$$\mathbb{B}_g(\mathbb{V}_i) = \left\{x \in \mathbb{R}^{9\times 1} : \|x\|_\infty \le L(\mathbb{X}_i) \max_{e_{vi}\in\mathbb{V}_i} \|e_{vi}\|_2\right\}.$$

Then, the augmented error system in (10) can be rewritten as

$$e_i(k+1) = A_{ei}e_i(k) + \tilde{w}_{ei}(k) \tag{12}$$

where $\tilde{w}_{ei} = e_{g_i}(k) + B_{ei}w_{ei}(k)$, and thus $\tilde{w}_{ei} \in \widetilde{\mathbb{W}}_{ei} = \mathbb{B}_g(\mathbb{V}_i) \oplus B_{ei}\mathbb{W}_{ei}$.

Assume that $\mathbb{Z}_i$ is a robustly positively invariant (RPI) set [26] with respect to system (12), *i.e.*,

$$A_{ei}e_i(k) + \tilde{w}_{ei}(k) \in \mathbb{Z}_i,\ \forall e_i(k) \in \mathbb{Z}_i,\ \forall \tilde{w}_{ei}(k) \in \widetilde{\mathbb{W}}_{ei}. \tag{13}$$

We can infer from (13) that if the involved parameters to be optimized are properly tuned, the feedback term and the disturbance compensation term can make the error system (12) tend to be stable.

B. Distributed MPC Feedforward Control

The feedforward control $\bar{u}_i(k)$ in (5) of ith vehicle is determined using a distributed MPC algorithm with the information transmitted from other controllers. Let $\bar{x}_i^*(k|t)$ is the nominal optimal trajectory of ith vehicle at time t. To achieve multi-objective control, several specifications are taken into account in the MPC optimization problem, including the safety distance between ith vehicle and adjacent ones, the stability of the vehicle platoon, the acceleration smoothness, and the fuel economy.

1) Design of DMPC Algorithm: For each vehicle i, the state of the nominal system (3) to be optimized is defined as

$$\bar{\xi}_i(t) = \beta \cdot \bar{x}_i(t),$$

with

$$\beta = \begin{bmatrix}1 & 0 & 0\\ 0 & 1 & 0\end{bmatrix}.$$

Here, the same sizes of the prediction horizon N_p and the control horizon N_c are used in each local control problem. Over any predictive horizon $[t,\ t+N_p]$, we denote three following types of state trajectory:

$$\begin{aligned}&\bar{\xi}_i^p(k|t) : \text{predicted state trajectory}\\ &\bar{\xi}_i^*(k|t) : \text{optimal state trajectory}\\ &\bar{\xi}_i^a(k|t) : \text{assumed state trajectory}\end{aligned}$$

where $k \in [0,\ N_p]$. $\bar{\xi}_i^p(k|t)$ is used as a trajectory variable to parameterize the local optimal control problem. $\bar{\xi}_i^*(k|t)$ denotes the optimal trajectory obtained by solving the optimal problem. $\bar{\xi}_i^a(k|t)$ is the assumed trajectory transmitted from vehicle i to vehicle $i+1$. Then, the cost function of the distributed MPC algorithm can be defined as

$$\begin{aligned}\mathscr{J}_i(t) &= \mathscr{J}_i(\bar{\xi}_i(t), \bar{u}_i(t))\\ &= \sum_{k=0}^{N_p-1} J_i(\bar{\xi}_i(k|t), \bar{u}_i(k|t)),\end{aligned} \tag{14}$$

where

$$\begin{aligned} J_i(\bar{\xi}_i(k|t), \bar{u}_i(k|t)) = &\|\bar{\xi}_i(k|t) - \bar{\xi}_{\text{des},i}(k|t)\|_{Q_i} \\ &+ \|\bar{\xi}_i(k|t) - \bar{\xi}^a_{i-1}(k|t) + d_{\text{des}}\|_{R_i} \\ &+ \|\bar{\xi}_i(k|t) - \bar{\xi}^a_i(k|t)\|_{G_i} \\ &+ \|a_i(\bar{\xi}_i(k|t))\|_{F_i}, \end{aligned}$$

and $\bar{\xi}_{\text{des},i}(k|t) = [\bar{\xi}^a_0(k|t) - i \cdot d_{\text{des}}]^\top$ is the desired position for ith vehicle, $d_{\text{des}} = [\, d_0, 0\,]^\top$ is the desired spacing, Q_i, R_i, G_i, F_i are the positive semi-definite weighting matrices.

The safety constraints for vehicle platoons should be also guaranteed with the following constraints:

$$\begin{aligned} &|p_i(k|t) - p_{i-1}(k|t) + d_0| < p_b, \\ &|v_i(k|t) - v_{i-1}(k|t)| < v_b, \\ &|a_i(k|t) - a_{i-1}(k|t)| < a_b, \end{aligned} \tag{15}$$

for $k = 0, 1, \ldots, N_p$. The constraints in (15) can be rewritten in a compact form

$$h(x_i(k|t), u_i(k|t)) \in \mathbb{H}_i,$$

where the bounded set $\mathbb{H}_i$ can be easily defined with d_0, p_b, v_b and a_b. Given an RPI set $\mathbb{Z}_i$ for system (12), the RPI subset $\mathbb{Z}_{xi}$ corresponding to the vehicle state x_i can be derived from $\mathbb{Z}_i$. Then, the constraints of the nominal system (3) can be computed as

$$\begin{aligned} \bar{x}_i(k|t) &\in \bar{\mathbb{X}}_i = \mathbb{X}_i \ominus \mathbb{Z}_{xi}, \\ \bar{u}_i(k|t) &\in \bar{\mathbb{U}}_i = \mathbb{U}_i \ominus K_i\mathbb{Z}_{xi} \ominus \mathbb{W}_i, \\ h(\bar{x}_i(k|t), \bar{u}_i(k|t)) &\in \bar{\mathbb{H}}_i = \mathbb{H}_i \ominus H_i\mathbb{Z}_{xi}. \end{aligned} \tag{16}$$

where $H_i = \text{diag}(2, 2, \frac{2\eta_i}{m_i r_i})$. The feedforward control design for ith vehicle can be now formulated as the following optimization problem:

$$\min_{\bar{u}^p_i} \mathscr{J}_i(t) \tag{17}$$

such that

$$\begin{aligned} &\bar{x}^p_i(k+1|t) = A_i\bar{x}^p_i(k|t) + g_i(\bar{x}^p_i(k|t)) + B_i\bar{u}^p_i(k|t) + G_i \\ &\bar{\xi}^p_i(k|t) = \beta \cdot \bar{x}^p_i(k|t) \\ &\bar{x}^p_i(k|t) \in \bar{\mathbb{X}}_i \\ &\bar{u}^p_i(k|t) \in \bar{\mathbb{U}}_i,\ k = 0, 1, \ldots, N_c - 1 \\ &\bar{u}^p_i(k|t) = \bar{u}^p_i(k-1|t),\ k = N_c, \ldots, N_p - 1 \\ &h(\bar{x}^p_i(k|t), \bar{u}^p_i(k|t)) \in \bar{\mathbb{H}}_i \\ &\bar{\xi}^p_i(N_p|t) = \bar{\xi}_{\text{des},i}(N_p|t) \\ &\bar{T}^p_i(N_p|t) = \frac{m_i r_i}{\eta_i} a_{fi}(\bar{v}^p_i(N_p|t)). \end{aligned} \tag{18}$$

Algorithm 1: The DMPC algorithm designed for vehicle i is shown as follows.

Initialization: At time $t < 0$, all the follower vehicles receive the new desired speed and spacing from the leader vehicle, and solve their local optimal problem (17) with $R_i = 0, G_i = 0$, for time $t = 0$. The initial optimal trajectory of the nominal system (3) at time $t = 0$ is calculated as

$$\bar{x}^*_i(k+1|0) = A_i\bar{x}_i(k|0) + g_i(\bar{x}_i(k|0)) + B_i\bar{u}_i(k|0) + G_i,$$

for $k = 0, 1, \ldots, N_p - 1$. Meanwhile, the first set of information has been transmitted to other vehicles as

$$\bar{x}^a_i(k|1) = \bar{x}^*_i(k+1|0),\ k = 0, 1, \ldots, N_p - 1.$$

Iteration: At any time $t > 0$, all vehicles follow the following steps to calculate the feedforward control.

Step 1: Apply $\bar{u}^*_i(0|t)$ for the nominal system (3).

Step 2: Compute the optimal state by using the current nominal state $\bar{x}_i(t)$ and the optimal control input $\bar{u}^*_i(0|t)$ in prediction horizon

$$\begin{aligned} \bar{x}^*_i(k+1|t) = &A_i\bar{x}^*_i(k|t) + g_i(\bar{x}^*_i(k|t)) \\ &+ B_i\bar{u}^*_i(k|t) + G_i \\ &k = 0, 1, \ldots, N_p - 1 \\ \bar{x}^*_i(0|t) = &\bar{x}_i(t) \\ \bar{\xi}^*_i(k|t) = &\beta \cdot \bar{x}^*_i(k|t). \end{aligned}$$

Step 3: Compute the assumed trajectory $\bar{x}^a_i(k|t+1)$ and the control input $\bar{u}^a_i(k|t+1)$ for next step

$$\begin{aligned} &\bar{x}^a_i(k|t+1) \\ &= \begin{cases} \bar{x}^*_i(k+1|t), & k = 0, 1, \ldots, N_p - 2 \\ \bar{x}^*_0(N_p|t) + i \cdot d_{\text{des}}, & k = N_p - 1 \end{cases} \end{aligned} \tag{19}$$

$$\begin{aligned} &\bar{u}^a_i(k|t+1) \\ &= \begin{cases} \bar{u}^*_i(k+1|t), & k = 0, 1, \ldots, N_p - 2 \\ \frac{m_i r_i}{\eta_i} a_{fi}(\bar{v}^*_i(N_p|t)), & k = N_p - 1 \end{cases} \end{aligned} \tag{20}$$

Step 4: Transmit $\bar{x}^a_i(\cdot|t+1)$ to the follower vehicle $i+1$, and receive the assumed trajectory from the connected vehicle (predecessor and leader vehicle).

Step 5: Solve the optimal problem (17) with the new information to get the $\bar{u}^*_i(\cdot|t+1)$.

Step 6: At the time $t+1$, select the control input $u^*_i(0|t+1)$ to ith vehicle and return to Step 1 for the next iteration.

To reduce the computational burden, we adopt the *Warm-Start* method in [39] for the optimization problem, which means that the solution at time t is used as the initial solution at time $t+1$ as indicated in (20). This method can effectively increase the computational efficiency, especially for nominal systems that are not affected by disturbances.

2) Recursive Feasibility Analysis of DMPC: Before proving the recursive feasibility of the optimization problem (17), a required condition is shown in the following theorem.

Theorem 1: [16] If the platoon system communication topology contains a spanning tree at the leader like the topologies shown in the Fig. 2, the terminal state in the predictive horizon N_p of the optimal problem (17) converges to the desired state in at most N steps, that is

$$\bar{\xi}^p_i(N_p|t) = \bar{\xi}_{\text{des},i}(N_p|t), \quad t \geq N.$$

Hence, an initial feasible assumption needs to be stated, which has been widely discussed in previous studies [16], [17].

Lemma 1: For the nominal system (3) of ith vehicle with a perfect state measurement and without disturbance, the feasibility of the open-loop optimal control problem (17) with equation

(14) subject to constrains (18) at time $t = 0$ implies its feasibility for all $t > 0$.

Proof: It is assumed that the optimal solution $\bar{u}_i^*(\cdot|t)$ is found at time t. The feedforward control $\bar{u}_i^*(\cdot|t)$ is held constant for the nominal system (3) after the control horizon N_c. Then, we can write $\bar{u}_i^*(k|t) = \bar{u}_{\text{ss},i}, (k \geq N_c)$ for this steady-state value. Consider the system dynamics, we define the steady-state $\bar{v}_{\text{ss},i}$ and $\bar{T}_{\text{ss},i}$ as the (in this case, unique) solutions of

$$\bar{v}_{\text{ss},i} = \bar{v}_{\text{ss},i} + \left(\frac{\eta_i}{m_i r_i} \bar{T}_{\text{ss},i} - a_f\left(\bar{v}_{\text{ss},i}\right) \right) \Delta t$$

$$\bar{T}_{\text{ss},i} = \bar{T}_{\text{ss},i} + \left(\bar{u}_{\text{ss},i} - \bar{T}_{\text{ss},i} \right) \frac{\Delta t}{\tau_i}$$

which are $\bar{T}_{\text{ss},i} = \bar{u}_{\text{ss},i}$ and $\bar{v}_{\text{ss},i} = a_f^{-1}(\frac{\eta}{mr}\bar{T}_{\text{ss},i})$. Note that for $\bar{u}_{\text{ss},i} > 0$ and hence $\bar{v}_{\text{ss},i} > 0$, this is an asymptotically stable equilibrium, and the domain of attraction includes all $v \in \mathbb{R}$, all $T \in \mathbb{R}$. The position $\bar{p}_i(k|t)$ will not converge to an equilibrium, but if we change variables $\tilde{p}_i(k|t) = \bar{p}_i(k|t) - k\bar{v}_{\text{ss},i}\Delta t$, we can write

$$\begin{aligned} &\bar{p}_i(k+1|t) - (k+1)\bar{v}_{\text{ss},i}\Delta t \\ &\quad = \bar{p}_i(k|t) - k\bar{v}_{\text{ss},i}\Delta t + \left(\bar{v}_i(k|t) - \bar{v}_{\text{ss},i}\right)\Delta t \end{aligned}$$

and thus

$$\tilde{p}_i(k+1|t) = \tilde{p}_i(k|t) + \left(\bar{v}_i(k|t) - \bar{v}_{\text{ss},i}\right)\Delta t.$$

This new position variable will also converge to a steady-state $\tilde{p}_{\text{ss},i}$ as $(\bar{v}_i(k|t) - \bar{v}_{\text{ss},i}) \to 0$. We will write $h, \tilde{x}_i = [\tilde{p}_i, \bar{v}_i, \bar{T}_i]^\top$ to denote the constraint function and system state accounting for this change of variables.

As we have shown that the system approaches the equilibrium, for $k = N_c, \ldots, N_p$, we have the set as

$$S_i = \left\{ \tilde{x}_i \in \mathbb{R}^3 \left| \begin{array}{l} \tilde{p}_i(k+1) = \tilde{p}_i(k) + \left(\bar{v}_i(k) - \bar{v}_{\text{ss},i}\right)\Delta t \\ \bar{v}_i(k+1) = \bar{v}_i(k) + \left(\frac{\eta_i}{m_i r_i}\bar{T}_i(k) - a_f\left(\bar{v}_i(k)\right) \right)\Delta t \\ \bar{T}_i(k+1) = \bar{T}_i(k) + \left(\bar{u}_{\text{ss},i} - \bar{T}_i(k)\right)\frac{\Delta t}{\tau_i} \\ \bar{u}_i(k) = \bar{u}_i(k-1) \\ h\left(\tilde{x}_i(k), \bar{u}_i(k)\right) \in \mathbb{H} \end{array} \right. \right\}.$$

The set S is an invariant set with respect to the dynamics of $\tilde{x}_i$ with the optimal solution $(\tilde{x}_i^*(\cdot|t), \bar{u}_i^*(\cdot|t))$ at time t. We will construct an $(\tilde{x}_i(\cdot|t+1), \bar{u}_i(\cdot|t+1))$ satisfying constraints at time $t+1$. For simplicity, we first assume that $\tilde{\xi}_{\text{des},i}$ has not changed from time t to $t+1$, and then modify our constructed solution to account for possible changes in $\tilde{\xi}_{\text{des},i}$.

Considering $(\tilde{x}_i(k|t+1), \bar{u}_i(k|t+1))$, for $k = 0, \ldots, N_p - 1$, all constraints in the optimisation problem at time $t+1$ are trivially satisfied by choosing the control input as (20) because these constraints are identical to constraints from time t. For prediction time $k = N_p$, we choose the control input as

$$\begin{aligned} \bar{u}_i(N_p - 1|t+1) &= \bar{u}_i^*(N_p - 2|t+1) \\ &= \frac{m_i r_i}{\eta_i} a_{fi}(\bar{v}_i^*(N_p|t)) \\ &= \frac{m_i r_i}{\eta_i} a_{fi}(\bar{v}_i(N_p - 1|t+1)). \end{aligned} \tag{21}$$

With the terminal state $\bar{x}_i^*(N_p|t)$ constrained by (18), we have

$$\begin{aligned} \bar{T}_i(N_p - 1|t+1) &= \bar{T}_i^*(N_p|t) \\ &= \frac{m_i r_i}{\eta_i} a_{fi}(\bar{v}_i^*(N_p|t)) \\ &= \frac{m_i r_i}{\eta_i} a_{fi}(\bar{v}_i(N_p - 1|t+1)). \end{aligned} \tag{22}$$

Then, combining equations (21) and (22), the terminal state $\tilde{x}_i$ of the system at time $t+1$ can be obtained as

$$\begin{aligned} \tilde{p}_i(N_p|t+1) &= \tilde{p}_i(N_p - 1|t+1) = \tilde{p}_{\text{ss},i} \\ \bar{v}_i(N_p|t+1) &= \bar{v}_i(N_p - 1|t+1) = \bar{v}_{\text{ss},i} \\ \bar{T}_i(N_p|t+1) &= \bar{T}_i(N_p - 1|t+1) = \bar{T}_{\text{ss},i} \end{aligned}$$

The nominal system state $\bar{x}_i$ can be obtained by choosing $\bar{p}_i(k|t) = \tilde{p}_i(k|t) + k\bar{v}_{\text{ss},i}$. Because S_i is an invariant set, which incorporates the constraint set $\mathbb{H}$, this choice satisfies all constraints (18) on $\bar{x}_i(N_p|t), \bar{u}_i(N_p|t)$.

Finally, we must account for possible changes in the communicated preceding vehicle states $\tilde{\xi}_{\text{des}}$. If these states have changed, the preceding vehicle acceleration $\bar{a}(k)$ has changed for some k. Defining $\delta\bar{a}(k)$ as this change, then let $\delta\bar{v}(k+1) = \delta\bar{v}(k) + \delta\bar{a}(k)\Delta t$ and $\delta\bar{p}(k+1) = \delta\bar{p}(k) + \delta\bar{v}(k)\Delta t$, for all k. We modify our constructed $\bar{x}(k)$ as

$$\begin{aligned} \bar{a}(k) &\mapsto \bar{a}(k) + \delta\bar{a}(k) \\ \bar{v}(k) &\mapsto \bar{v}(k) + \delta\bar{v}(k) \\ \bar{p}(k) &\mapsto \bar{p}(k) + \delta\bar{p}(k) \end{aligned}$$

and choose $\bar{u}(k)$ consistently with this change in $\bar{a}(k)$. This leaves the differences $\bar{p}_i(k) - \bar{p}_{i-1}(k), \bar{v}_i(k) - \bar{v}_{i-1}(k), \bar{a}_i(k) - \bar{a}_{i-1}(k)$ unchanged since the changes in $\tilde{\xi}_{\text{des}}$ is transmitted from the leader to all followers (directly or indirectly). Hence, we satisfy the constraints $h(\tilde{x}(k), \bar{u}(k)) \in \mathbb{H}$ at time $t+1$ if they were satisfied at t. ■

3) Stability Analysis of DMPC: We now prove the stability of the platoon system by analyzing the decreasing properties of the platoon cost function. To this end, the sum of the optimal cost functions is defined as

$$\begin{aligned} \mathscr{J}_\Sigma^*(t) &= \sum_{i=1}^{N} \mathscr{J}_i^*(\bar{\xi}_i^*(\cdot|t), \bar{\xi}_{-i}^a(\cdot|t), \bar{u}_i^*(\cdot|t)) \\ &= \sum_{k=0}^{N_p - 1} L(\bar{\xi}^*(k|t), \bar{\xi}^a(k|t), \bar{u}^*(k|t)) \end{aligned} \tag{23}$$

where

$$\begin{aligned} L(\bar{\xi}, \bar{\xi}^a, \bar{u}) = \sum_{i=1}^{N} (&\|\bar{\xi}_i - \bar{\xi}_{\text{des},i}\|_{Q_i} + \|\bar{\xi}_i - \bar{\xi}_{i-1}^a + d_{\text{des}}\|_{R_i} \\ &+ \|\bar{\xi}_i - \bar{\xi}_i^a\|_{G_i} + \|a_i(\bar{\xi}_i)\|_{F_i}). \end{aligned}$$

With the terminal state $\bar{\xi}_i^p(N_p|t) = \bar{\xi}_{\text{des},i}(N_p|t)$, $t \geq N$ provided by Theorem 1, and the feasible control $u_i^p(\cdot|t) = u_i^a(\cdot|t)$ provided by Algorithm 1, the distributed optimal cost function can be bounded as

$$\begin{aligned}\mathscr{J}_\Sigma^*(t+1) &\le \sum_{k=0}^{N_p-1} L(\bar{\xi}^a(k|t+1), \bar{\xi}^a(k|t+1), \bar{u}^a(k|t+1)) \\ &= \sum_{k=0}^{N_p-2} L(\bar{\xi}^*(k+1|t), \bar{\xi}^*(k+1|t), \bar{u}^*(k+1|t)).\end{aligned} \tag{24}$$

The equality holds due to the definitions of $\bar{x}_i^a(k|t+1)$ and $\bar{u}_i^a(k|t+1)$ in (19) and (20), respectively. Subtracting the equation (23) from (24) yields

$$\begin{aligned}&\mathscr{J}_\Sigma^*(t+1) - \mathscr{J}_\Sigma^*(t) \\ &\quad\le \sum_{k=1}^{N_p-1} L(\bar{\xi}^*(k|t), \bar{\xi}^*(k|t), \bar{u}^*(k|t)) \\ &\quad\quad - \sum_{k=0}^{N_p-1} L(\bar{\xi}^*(k|t), \bar{\xi}^a(k|t), \bar{u}^*(k|t)) \\ &\quad= -L(\bar{\xi}^*(0|t), \bar{\xi}^a(0|t), \bar{u}^*(0|t)) + \sum_{k=1}^{N_p-1} \Delta_k\end{aligned}$$

where

$$\begin{aligned}\Delta_k &= L(\bar{\xi}^*(k|t), \bar{\xi}^*(k|t), \bar{u}^*(k|t)) \\ &\quad - L(\bar{\xi}^*(k|t), \bar{\xi}^a(k|t), \bar{u}^*(k|t)) \\ &= \sum_{i=1}^{N} (\|\bar{\xi}_i^*(k|t) - \bar{\xi}_{\text{des},i}(k|t)\|_{Q_i} \\ &\quad + \|\bar{\xi}_i^*(k|t) - \bar{\xi}_{i-1}^*(k|t) + d_{\text{des}}\|_{R_i} \\ &\quad + \|\bar{\xi}_i^*(k|t) - \bar{\xi}_i^*(k|t)\|_{G_i} + \|a_i(\bar{\xi}_i^*(k|t))\|_{F_i}) \\ &\quad - \sum_{i=1}^{N} (\|\bar{\xi}_i^*(k|t) - \bar{\xi}_{\text{des},i}(k|t)\|_{Q_i} \\ &\quad + \|\bar{\xi}_i^*(k|t) - \bar{\xi}_{i-1}^a(k|t) + d_{\text{des}}\|_{R_i} \\ &\quad + \|\bar{\xi}_i^*(k|t) - \bar{\xi}_i^a(k|t)\|_{G_i} + \|a_i(\bar{\xi}_i^*(k|t))\|_{F_i}).\end{aligned} \tag{25}$$

Using the triangle inequality for vector norms with $R_1 = 0$, the term Δ_k defined in (25) is bounded as

$$\Delta_k \le \sum_{i=1}^{N-1} (\|\bar{\xi}_i^*(k|t) - \bar{\xi}_i^a(k|t)\|_{R_{i+1}} - \|\bar{\xi}_i^*(k|t) - \bar{\xi}_i^a(k|t)\|_{G_i}).$$

Then, the weights of the cost function (14) can be designed as follows:

$$G_i \ge R_{i+1},\ i = 0, 1, \ldots, N-1. \tag{26}$$

It follows from (26) that the function $\mathscr{J}_\Sigma^*(\cdot)$ satisfies

$$\mathscr{J}_\Sigma^*(t+1) - \mathscr{J}_\Sigma^*(t) \le -L(\bar{\xi}^*(0|t), \bar{\xi}^a(0|t), \bar{u}^*(0|t)). \tag{27}$$

Inequality (27) shows that the platoon cost function $\mathscr{J}_\Sigma^*(\cdot)$ is strictly monotonically decreasing. Thus, the asymptotic stability of the platoon system can be guaranteed.

From the above analysis, the states of the nominal system will asymptotically converge to the desired states as

$$\lim_{k\to\infty} \begin{bmatrix} \bar{p}_i(k) - \bar{p}_0(k) + i \cdot d_0 \\ \bar{v}_i(k) - \bar{v}_0(k) \\ \bar{a}_i(\bar{x}_i(k)) \end{bmatrix} = \begin{bmatrix} 0 \\ 0 \\ 0 \end{bmatrix}.$$

Then, the states of the actual vehicle system will achieve the objective (4) with a set value of σ_i defined as

$$\sigma_i = \begin{bmatrix} 2 & 0 & 0 \\ 0 & 2 & 0 \\ 0 & 0 & \frac{\eta_i}{m_i r_i} \end{bmatrix} \mathbb{Z}_{xi}.$$

IV. Integrated Control Design Procedure

This section presents the design of both unknown input observer and feedback control. The implementation of the proposed distributed MPC control scheme is also discussed.

A. Offline Computation

Hereafter, PSO algorithm is exploited to design both observer and feedback gains. Then, the RPI set of the extended error system (12) and the constraints (16) of the vehicle nominal system (3) are determined.

1) PSO-Based Control Feedback Design: The following specifications are taken into account in the design of both observer and control feedback gains:

- the stability of the augmented error system (12) under the effect of bounded disturbance w_{ei},
- the size of the RPI sets $\mathbb{Z}_{xi}$ and $K_i\mathbb{Z}_{xi}$ of system (12).

To minimize the effect of the disturbance, the $\mathscr{H}_\infty$ performance is taken into account in the design of both the feedback control gain and the observer gain. To this end, we consider the controlled output $z_i(k) = Ex_i(k)$ associated to system (12), where E is selected as $\text{diag}(100, 1, 0.01\ 100, 1, 0.01, 0, 0, 0)$. Using the bounded real lemma [40], the following theorem provides conditions to guarantee an $\mathscr{H}_\infty$ control performance for the closed-loop system (12).

Theorem 2: If there exit a positive definite matrix M_i, matrices K_i, L_{Pi}, L_{I1i}, L_{I2i}, L_{I3i}, of appropriate dimensions, and a positive scalar γ_i such that the following optimization problem is achievable:

$$\min_{P_i=\{K_i, L_{Pi}, L_{I1i}, L_{I2i}, L_{I3i}\}} \gamma_i$$

such that

$$\begin{bmatrix} A_{ei}^\top M_i A_{ei} - M_i & A_{ei}^\top M_i B_{ei} & E^\top \\ * & B_{ei}^\top M_i B_{ei} - \gamma_i^2 I & 0 \\ * & * & -I \end{bmatrix} < 0. \tag{28}$$

Then, system (12) is stable with an $\mathscr{H}_\infty$ performance level less than or equal to γ_i.

The optimization problem (28) in Theorem 2 is nonconvex due to the nonlinear couplings between decisions variables. Finding a solution for such a nonconvex problem is NP hard. Here, PSO algorithm is exploited to derive the optimal control feedback gain and the observer gains. Note that the initial gains $P_i(0)$ are obtained from linear quadratic regulator (LQR) and pole assignment methods. To reduce the computational burden, the particle position P_i and velocity V_i are constrained

$$P_{i,j}(n) \in [P_{\min},\, P_{\max}],\ j = 1, 2, \ldots, N_1,$$
$$V_{i,j}(n) \in [V_{\min},\, V_{\max}],\ n = 0, 1, \ldots, N_2,$$

where j is the particle number, N_1 is the total number of particles, n is the iterations, N_2 is the total number of iterations. The initial state of all search particles are given by

$$P_{i,j}(0) = P_{\min} + r_a\,(P_{\max} - P_{\min}),$$
$$V_{i,j}(0) = V_{\min} + r_a\,(V_{\max} - V_{\min}),$$

where r_a is a random number drawn from uniform distribution between 0 and 1. The position $P_{i,j}$ and the velocity $V_{i,j}$ are updated as [41]

$$P_{i,j}(n+1) = P_{i,j}(n) + V_{i,j}(n+1),$$
$$V_{i,j}(n+1) = w_a V_{i,j}(n) + c_1 r_{a1}(P_{i,j}^{pb}(n) - P_{i,j}(n)) + c_2 r_{a2}(P_i^{gb}(n) - P_{i,j}(n)),$$

where w_a is the inertia weight, $P_{i,j}^{pb}(n)$ is the best previous position of jth particle at iteration n, $P_i^{gb}(n)$ is the global best position in the swarm at iteration n, c_1 and c_2 are the accelerated constant, r_{a1} and r_{a2} are random numbers drawn from uniform distribution between 0 and 1. Note that after N_2 iterations, the optimal control parameters can be obtained as $P_i = P_i^{gb}(N_2)$.

2) Computation of Robustly Positive Invariant Set: The RPI set can be computed following the method in [31]. To this end, we define the following convex compact set $F_{s,i}$:

$$F_{s,i} = \bigoplus_{j=0}^{s-1} A_{ei}^j \widetilde{\mathbb{W}}_{ei},\ \text{with } F_{0,i} = \{0\}.$$

Note that the minimal RPI (mRPI) set, denoted by $F_{\infty,i}$, is given by

$$F_{\infty,i} = \bigoplus_{j=0}^{\infty} A_{ei}^j \widetilde{\mathbb{W}}_{ei}.$$

The following lemma is useful to compute the RPI set of system (12).

Lemma 2: [42] If $0 \in \widetilde{\mathbb{W}}_{ei}$. Then, there exists a finite integer $s \in \mathbb{N}_+$ and a scalar $\alpha \in [0, 1)$ satisfying

$$A_{ei}^s \widetilde{\mathbb{W}}_{ei} \subseteq \alpha \widetilde{\mathbb{W}}_{ei}. \tag{29}$$

If condition (29) holds, then there exists a convex compact RPI set

$$F(\alpha, s, i) = (1-\alpha)^{-1} F_{s,i}, \tag{30}$$

such that $0 \in F(\alpha, s, i)$ and $F_{\infty,i} \subseteq F(\alpha, s, i)$.

As shown in [31], the set $F(\alpha, s, i)$ defined in (30) is an outer approximation of the mRPI set $F_{\infty,i}$. Note that the smaller values of s and α lead to a better approximation of $F_{\infty,i}$. We denote the smallest values of s and α as

$$s^\circ(\alpha, i) = \min\{s \in \mathbb{N}_+ | A_{ei}^s \widetilde{\mathbb{W}}_{ei} \subseteq \alpha \widetilde{\mathbb{W}}_{ei}\},$$
$$\alpha^\circ(s, i) = \min\{\alpha \in \mathbb{R} | A_{ei}^s \widetilde{\mathbb{W}}_{ei} \subseteq \alpha \widetilde{\mathbb{W}}_{ei}\}.$$

In this paper, selecting $\alpha = 0.05$, we obtain $s_i = s^\circ(0.05, i)$ and $\alpha_i = \alpha^\circ(s^\circ(0.05, i))$. Then, the corresponding RPI set is computed as

$$\mathbb{Z}_i = F(\alpha_i, s_i, i) = F(\alpha^\circ(s^\circ(0.05, i)), s^\circ(0.05, i), i).$$

TABLE I
ENVIRONMENTAL SETTINGS

Parameters	Values	Parameters	Values
Δt_i	0.05	r_{ni}	rand(0,1)
η_i	0.95	N_p	12
m_i (kg)	1500+300r_{ni}	N_c	5
r_i (m)	0.3+0.1r_{ni}	p_b (m)	2
τ_i	0.1+0.1r_{ni}	v_b (m/s)	5
f_i	0.015+0.005r_{ni}	a_b (m/s^2)	5
θ_i ($^\circ$)	5+r_{ni}	Q_i	diag(100,1)
C_{Ai}	0.6+0.2r_{ni}	R_i	diag(50,0.5)
c_1	2	G_i	diag(100,1)
c_2	2	F_i	0.5
N_1	30	N_2	100
$v_{\min}$ (m/s)	0	$v_{\max}$ (m/s)	35
$a_{\min}$ (m/s^2)	-6	$a_{\max}$ (m/s^2)	6
$T_{\min}$ (Nm)	0	$T_{\max}$ (Nm)	1000
P_i	$\{[835, 427, 0.52]$,$[2.5, 41, 900]^\top$,33700,24800,8300$\}$		

TABLE II
SIMULATION CONDITIONS OF SCENARIO 1

Parameters \ Time (s)	$[0, i-1)$	$[i-1, 24+i)$	$[24+i, 50]$
d_0 (m)	20	20	20
v_0 (m/s)	20	20	20
w_i (N)	0	$500\sin(\frac{t-i+1}{2.9})$	375

TABLE III
OBSERVER PERFORMANCE COMPARISON

	ESO	P2IO	P3IO	P4IO
RMSE (N)	24.3	13.7	10.6	10.9

The multi-parametric toolbox (MPT) [43] can be used for the set computations.

3) Nominal Constraints Computation: After computing the invariant set $\mathbb{Z}_i$, the sets of tightened constraints $\bar{\mathbb{X}}_i$, $\bar{\mathbb{U}}_i$ and $\bar{\mathbb{H}}_i$ can be defined for the nominal vehicle system (3) from (16). Then, the designed integrated control law (5) can ensure the states x_i and control input u_i of ith vehicle to satisfy the constraints (15).

B. Online Control Implementation

Once the offline computations are finished, the online implementation steps are performed at the time $t \geq 0$ as follows.

Step 1: Use the output $y_i(t)$ and control input $u_i(t)$ of the ith vehicle to compute the estimated state $\hat{x}_i(t+1)$ and disturbance $\hat{w}_i(t+1)$ following (6).

Step 2: Compute the nominal system state $\bar{x}_i(t+1)$ using the nominal state $\bar{x}_i(t)$ and the control input $\bar{u}_i(t)$.

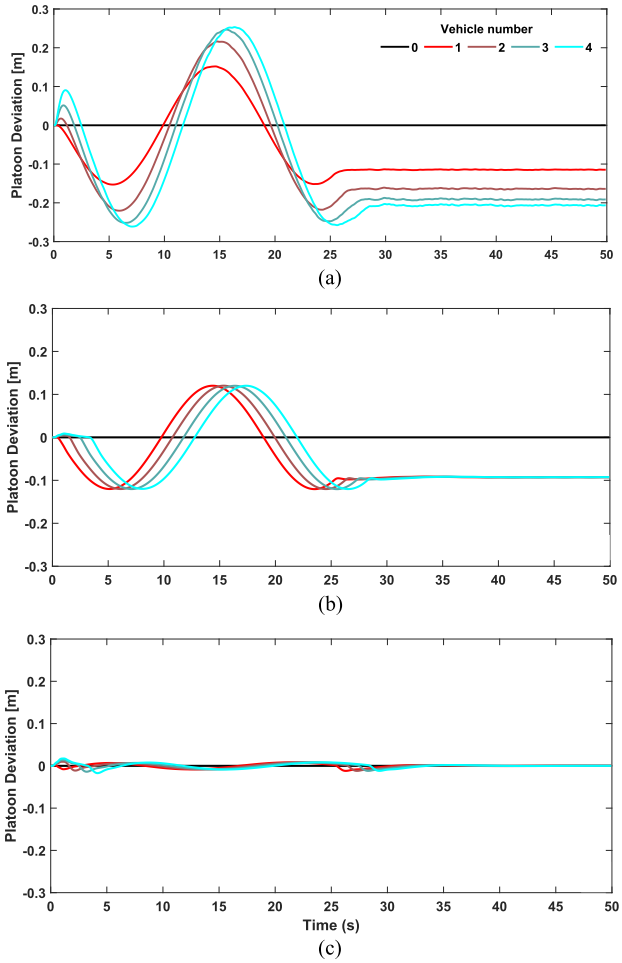

Fig. 4. Platoon deviation Δd_p. (a) Classical DMPC, (b) RNMPC in [30], (c) Proposed controller.

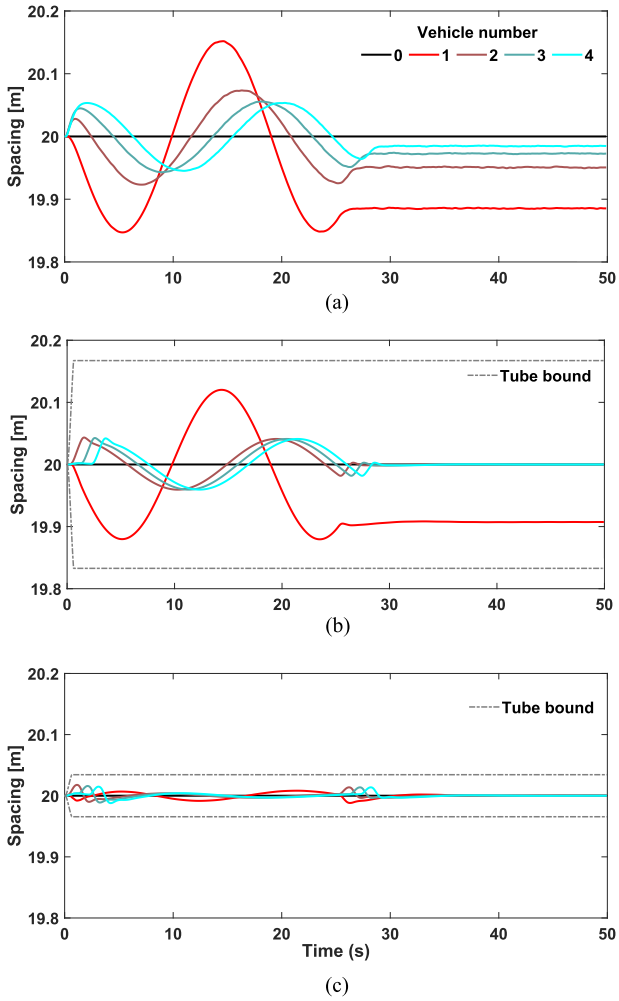

Fig. 5. Adjacent spacing d_s. (a) Classical DMPC, (b) RNMPC in [30], (c) Proposed controller.

TABLE IV
SIMULATION CONDITIONS OF SCENARIO 2

Parameters \ Time (s)	$[0,5)$	$[5,9)$	$[9,14)$	$[14,20)$	$[20,50]$
d_0 (m)	30	30	30	30	30
v_0 (m/s)	30	$30-3t$	18	$18+2t$	30
w_i (N)	$0,\ t\in[0,1.5i-1.5)$				
	$500\sin(\frac{t-1.5i+1.5}{4}),\ t\in[1.5i-1.5,50]$				

TABLE V
SUMMARY OF COMPARISON RESULTS

	Scenario 1			Scenario 2		
	Classical DMPC	Proposed controller	Relative improvement	Classical DMPC	Proposed controller	Relative improvement
Peak platoon deviation (m)	0.2615	0.0174	93.3%	0.3770	0.0411	89.1%
Average platoon deviation (m)	0.1317	0.0036	97.2%	0.1244	0.0057	95.4%
Computation time (s)	34.2	11.4	66.7%	40.9	17.3	57.7%
Communication number (/s)	20	10	50%	20	14	30%

Step 3: Compute the feedback control and disturbance-compensation control from the results of Steps 1 and 2.

Step 4: Run Algorithm 1 to obtain the optimal control sequence $[\bar{u}_i^*(0|t+1), \bar{u}_i^*(1|t+1), \ldots, \bar{u}_i^*(N_p-1|t+1)]$ for the nominal system.

Step 5: Select the first element $\bar{u}_i(0|t+1)$ from the optimal control sequence to use for feedforward control $\bar{u}_i(t+1)$. Then, compute the integrated control law $u_i(t+1)$ for ith vehicle by combining the results of Step 3.

$$u_i(t+1) = \bar{u}_i(t+1) + K_i(\hat{x}_i(t+1) - \bar{x}_i(t+1)) - B_i^{\dagger} H \hat{w}_i(t+1).$$

Step 6: At the time $t+1$, apply the control input $u_i(t+1)$ to ith vehicle and return to Step 1 for the next iteration.

V. SIMULATION AND COMPARISON RESULTS

This section provides simulation results obtained with two different scenarios and working conditions for vehicle platoons, composed of one leading vehicle and four following vehicles.

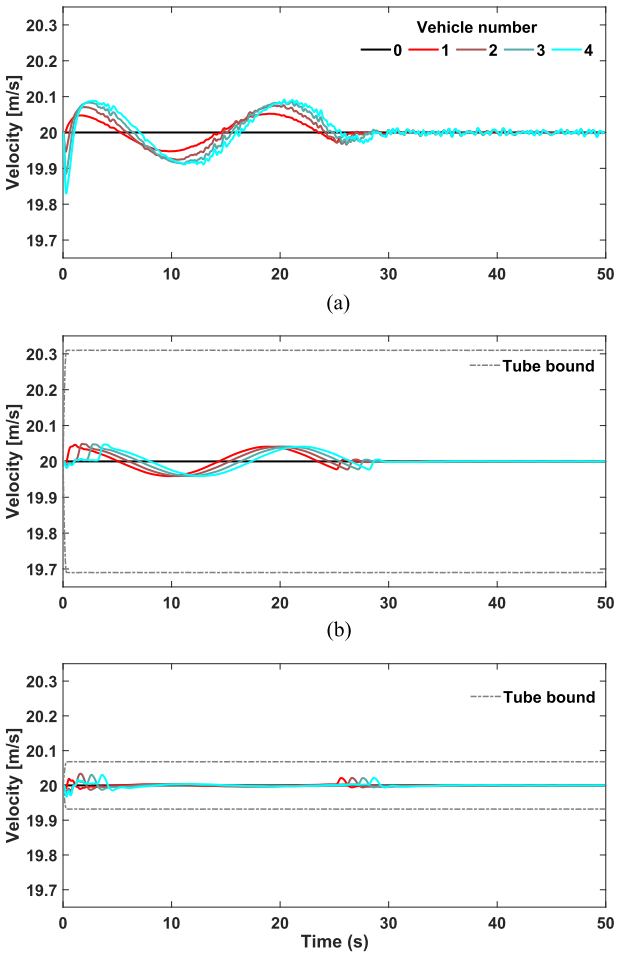

Fig. 6. Velocity of following vehicles. (a) Classical DMPC, (b) RNMPC in [30], (c) Proposed controller.

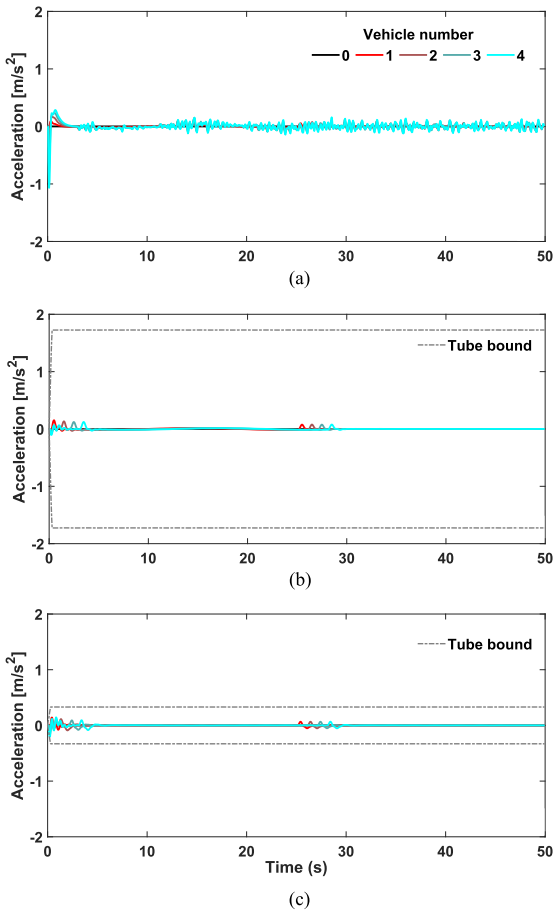

Fig. 7. Acceleration of following vehicles. (a) Classical DMPC, (b) RNMPC in [30], (c) Proposed controller.

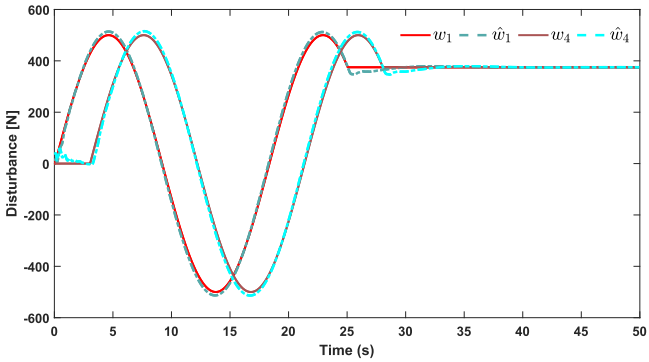

Fig. 8. Estimation of the lumped disturbance.

The proposed control method is compared with the classical DMPC control scheme [16] and tube-based robust nonlinear MPC (RNMPC) method [30]. These algorithms are implemented in a distributed way like Algorithm 1. The stabilizing state feedback gain of RNMPC method for the error system $e_{x_i} = x_i - \bar{x}_i$ between (2) and (3) will be selected as the infinite horizon LQR solution $K^{\infty}_{\mathrm{LQR},i}$ for system (A_i, B_i). Therefore, the RNMPC controller is designed as

$$u_{\mathrm{RNMPC},i} = \bar{u}_{\mathrm{RNMPC},i} + K^{\infty}_{\mathrm{LQR},i}(x_{\mathrm{RNMPC},i} - \bar{x}_{\mathrm{RNMPC},i}),$$

where $\bar{u}_{\mathrm{RNMPC},i}$ is the optimal control input for the nominal system (3), which is computed by solving a constrained finite-time optimal control problem with the cost function defined in (14). The $K^{\infty}_{\mathrm{LQR},i}$ is also used in the computation of the robust invariant set $\mathbb{Z}_{\mathrm{RNMPC},i}$:

$$F_{\mathrm{RNMPC}}(\alpha, s, i) = (1-\alpha)^{-1} F_{\mathrm{RNMPC},s,i}$$

$$= (1-\alpha)^{-1} \bigoplus_{j=0}^{s-1} (A_i + B_i K^{\infty}_{\mathrm{LQR},i})^j H \mathbb{W}_i$$

$$\mathbb{Z}_{\mathrm{RNMPC},i} = F_{\mathrm{RNMPC}}(\alpha^{\circ}(s^{\circ}(0.05, i)), s^{\circ}(0.05, i), i).$$

All controllers are implemented using MATLAB 2019a with Intel i5-8250U and 8G RAM. The environmental settings are described in Table I. The parameters of the heterogeneous vehicles are randomly selected according to the passenger vehicles. Then, the nominal vehicle model is different from the actual vehicle model.

A. Scenario 1: Performance Under Disturbance Effects

This test allows to compare the performance of different controllers under time-varying and time-invariant external disturbances. The simulation scenario and the working condition are specified in Table II.

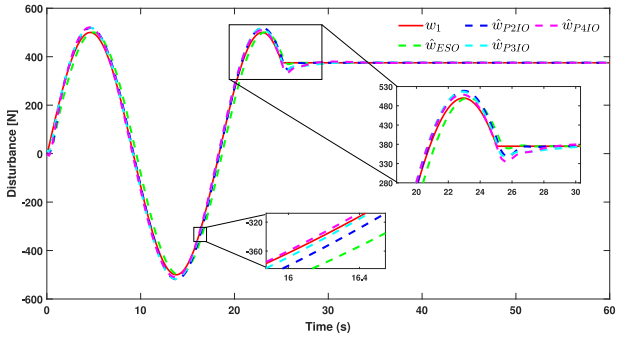

Fig. 9. Estimation of the lumped disturbance with different types of observers.

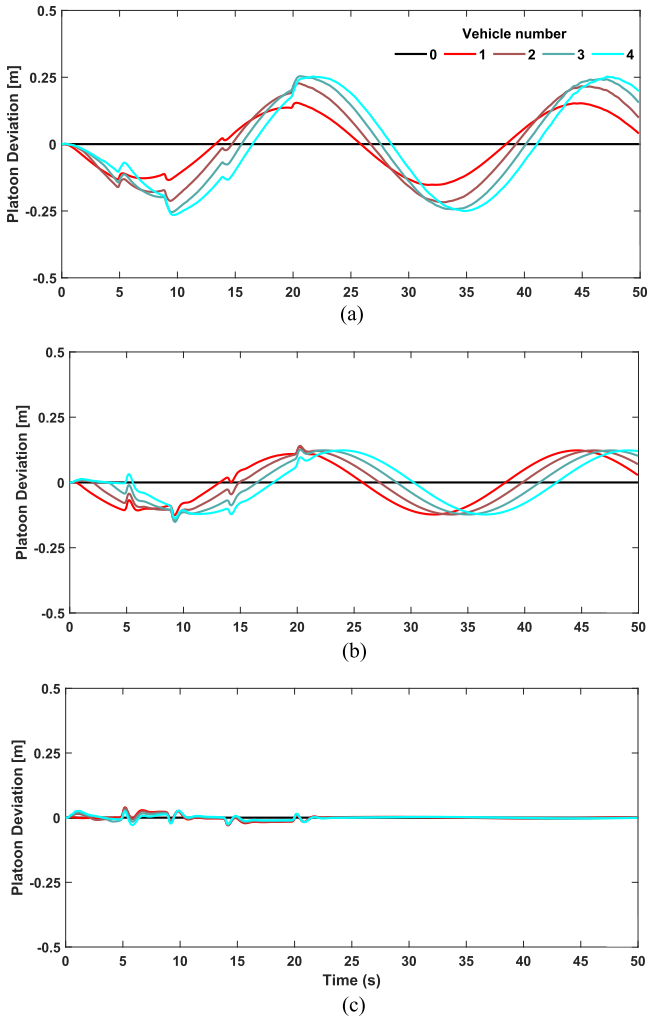

Fig. 10. Platoon deviation Δd_p. (a) Classical DMPC, (b) RNMPC in [30], (c) Proposed controller.

Fig. 4 shows that the proposed control scheme can compensate effectively the effects caused by the external disturbance. In the first 25 seconds, under the impact of the periodic disturbance, the platoon deviation induced by both control methods are fluctuating periodically. The amplitude of the classical DMPC method is ± 0.3 m, the RNMPC method is ± 0.13 m, while that of the proposed controller is only ± 0.02 m. Under the constant disturbance after 25 seconds, the DMPC and RNMPC algorithm

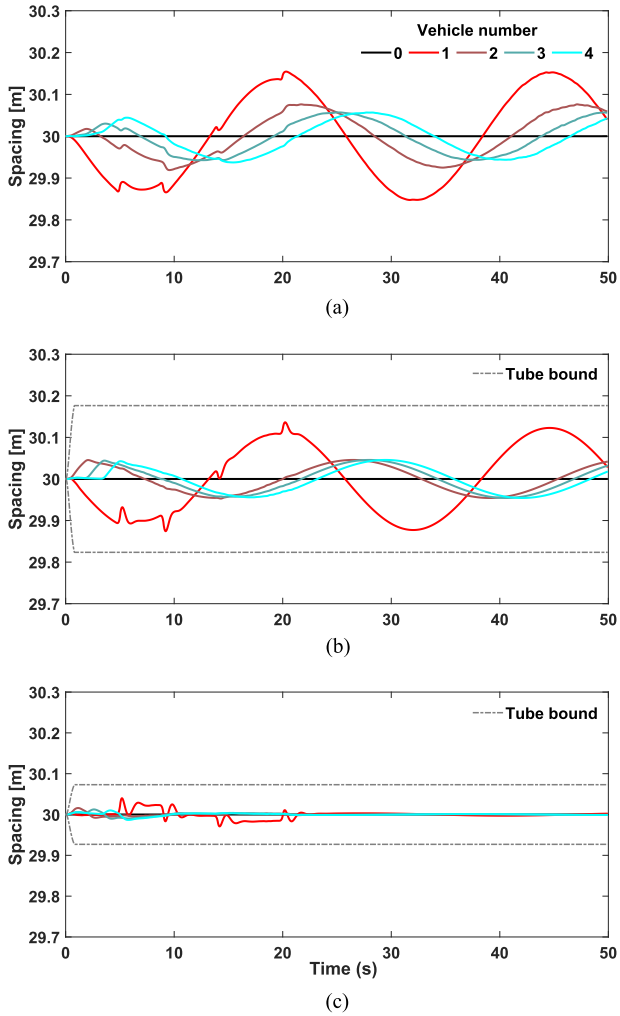

Fig. 11. Adjacent spacing d_s. (a) Classical DMPC, (b) RNMPC in [30], (c) Proposed controller.

leads to a static error, which is not the case of the proposed approach. Moreover, due to the presence of interference, the DMPC method cannot guarantee that the platoon deviation is not amplified as the vehicle number increased with the PLF communication topology even if the speed of the leading vehicle remains unchanged.

The control situation of vehicle spacing under two different controllers is shown in Fig. 5. It can be seen more intuitively that different static errors exist in each adjacent spacing with traditional DMPC, while the proposed controller has a good control effect for all vehicles. Figs. 6 and 7 present a comparison among three controllers in terms of vehicle velocity and acceleration. We can see that the DMPC introduces important oscillations due to disturbance effects and chattering can be observed in both speed and acceleration results. However, the disturbance effect is significantly minimized with the proposed controller, which induces no visible chattering phenomenon in both speed and acceleration results. Both the RNMPC and the proposed controller ensure that the states are within the invariant set of the nominal system. However, RNMPC has a larger boundary, which makes the controller unnecessarily conservative.

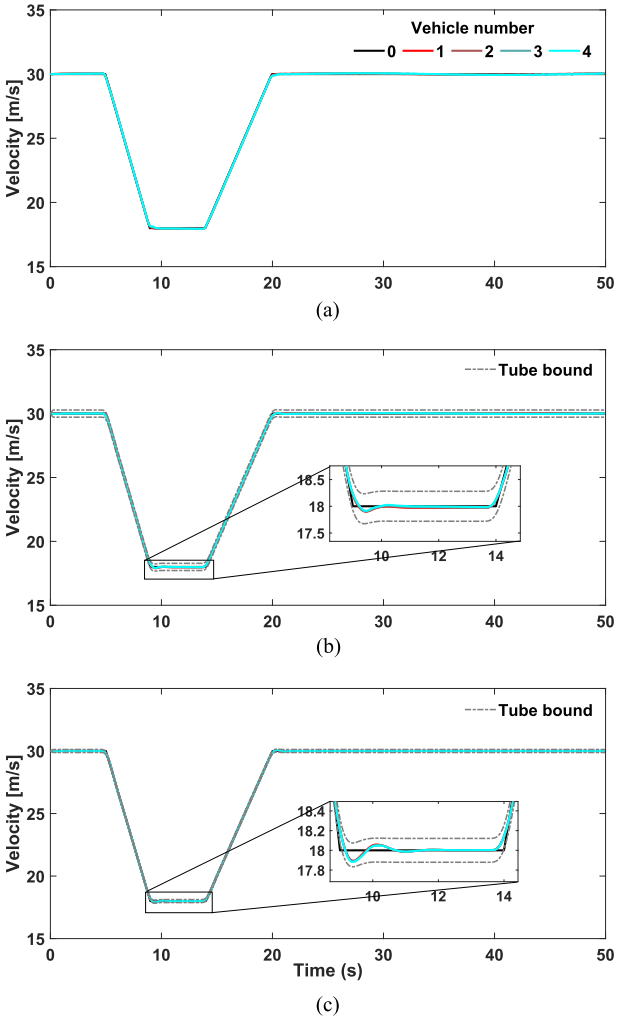

Fig. 12. Velocity of following vehicles. (a) Classical DMPC, (b) RNMPC in [30], (c) Proposed controller.

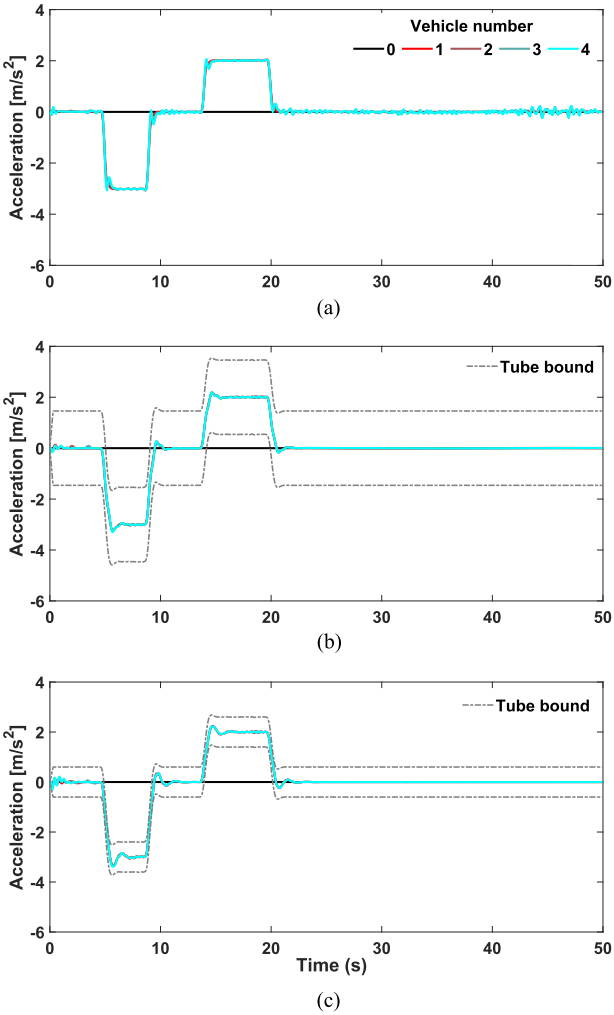

Fig. 13. Acceleration of following vehicles. (a) Classical DMPC, (b) RNMPC in [30], (c) Proposed controller.

For illustrations, Fig. 8 depicts the estimation of external disturbances for the first and the last following vehicles in the platoon. We can observe a high estimation performance can be obtained with the designed unknown input observer. This allows for an effective disturbance-compensation control action to improve the overall control performance of the proposed integrated control scheme. In addition, we also consider the comparison of different disturbance observers in the simulation as shown in Fig. 9, which includes PMI observers of different orders and an extended state observer (ESO). Note that PMI observer with an n-order disturbance model is denoted by PnIO in the figure. Furthermore, the root mean square error (RMSE), defined as

$$\text{RMSE} = \sqrt{\frac{1}{m}\sum_{t=1}^{m}\left[w(t) - \hat{w}(t)\right]^2},$$

is adopted as the evaluation index to compare the performance differences of the considered observers. The comparison results are shown in Table III.

As can be seen from Fig. 9, PMI observers perform better than ESO when dealing with time-varying disturbances. The results in Table III show that the higher-order observers P3IO and P4IO also have a slightly better performance over P2IO

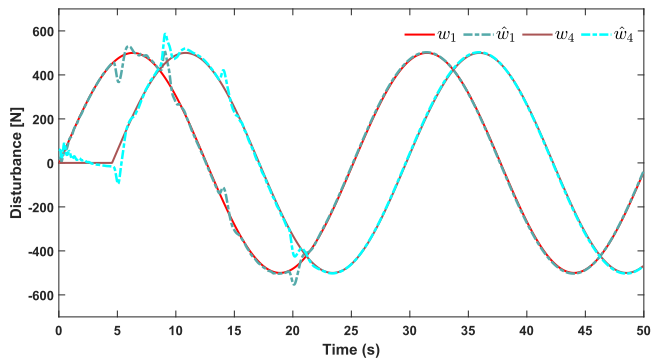

Fig. 14. Estimation of the lumped disturbances.

observer. However, the observer P4IO did not perform as well as expected due to a large number of involved parameters, which leads to difficulties in observer gain tuning.

B. Scenario 2: Performance Under Vehicle Acceleration and Deceleration

In this scenario, we set a variable speed of the leading vehicle in the presence of external disturbances. It is required that the following vehicles keep the spacing unchanged under

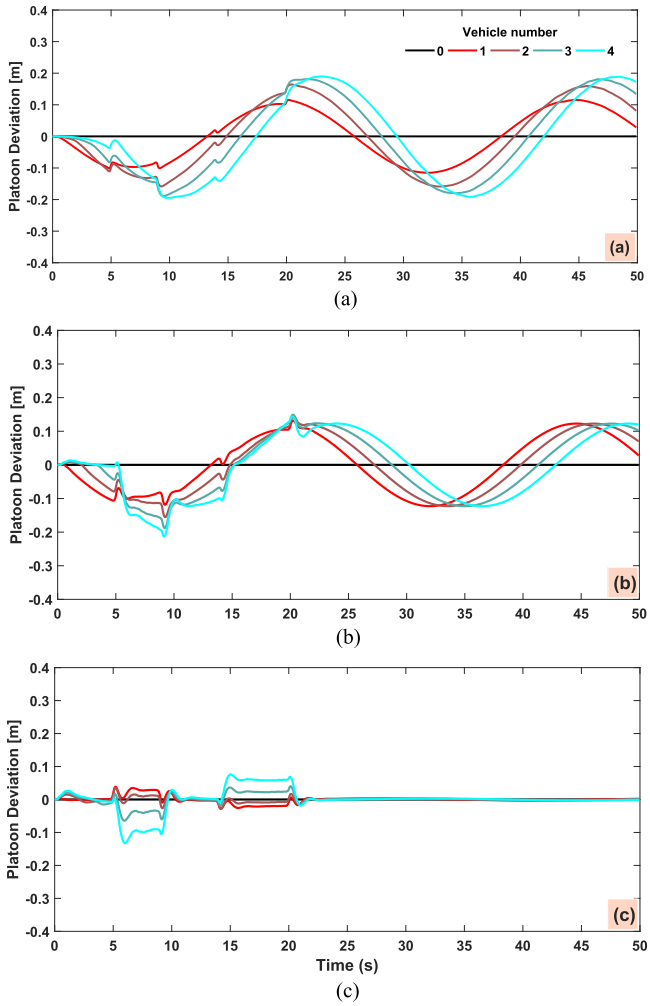

Fig. 15. Platoon deviation Δd_p (with PF communication topology). (a) Classical DMPC, (b) RNMPC in [30], (c) Proposed controller.

the condition that the leading vehicle status changes, so as to detect the control performance of the two controllers under acceleration/deceleration. The simulation conditions of this test scenario are shown in Table IV.

Fig. 10 shows the comparison of the platoon deviation Δd_p obtained with three controllers. In the first 20 seconds, all results show irregular variations in deviation. Note that the DMPC leads to a large error range of ± 0.4 m compared to that of the proposed controller (± 0.04 m). Moreover, after 20 seconds, the platoon derivation becomes very small only with the proposed controller. Similar remarks can be done for the spacing comparison in Fig. 11. Therefore, the state change of the leading vehicle greatly affects the control performance, but it is still controllable.

In this scenario, the vehicle state has a large change as shown in Figs. 12 and 13. However, under the action of the proposed controller, there is no visible chattering behavior in the states of the following vehicles as in the classical DMPC. Moreover, the vehicle state is constrained within a limited boundary during the whole test scenario. The disturbance estimation during the platoon mission change process is shown in Fig. 14. It can be seen that despite the acceleration and the deceleration conditions, the obtained estimation performance is still satisfactory. Note that for this simulation scenario, we also add a platoon control with different communication topologies. The obtained results are shown in Fig. 15, which also indicate an outperformance of the proposed controller compared to two other ones.

Due to the presence of disturbances, the classical DMPC method must transmit the controller information to the receiving vehicles several times in a short time, which also increases the computational burden. The data solved by DMPC in the proposed scheme are all from the nominal system, which can effectively reduce the communication number of times, the calculation time and the difficulty of solving. Moreover, the proposed controller has a better control effect for vehicle platoon as shown in Figs. 4 and 10. The test results of the above-mentioned data for both test scenarios are summarized in Table V. The comparative study shows a clear outperformance of the proposed controller compared to the classical DMPC scheme in [16].

VI. Conclusion

An integrated controller, including feedforward control, feedback control and disturbance-compensation control, has been proposed. This control law combines TMPC, PMI observer, and DMPC to ensure the stability of the vehicle platoon control, and effectively compensate the influence of lumped disturbances. The proposed control scheme exploits the main advantages, performs their respective functions, and complements each other. The proposed controller provides a faster solution speed than a classical DMPC scheme with unknown input. Moreover, our method leads to more reasonable constraint conditions and solution environment than RNMPC scheme, which allows obtaining a better control performance.

As a direction to extend this work, future research will further minimize the impacts of random communication delay in vehicle platoons. Additionally, more applicable scenarios of the proposed controller will be found in future works.

References

[1] K. Hedrick, M. Tomizuka, and P. Varaiya, "Control issues in automated highway systems," *IEEE Control Syst. Mag.*, vol. 14, no. 6, pp. 21–32, Dec. 1994.

[2] S. Shladover *et al.*, "Automated vehicle control developments in the PATH program," *IEEE Trans. Veh. Technol.*, vol. 40, no. 1, pp. 114–130, Feb. 1991.

[3] B. Van Arem, C. J. Van Driel, and R. Visser, "The impact of cooperative adaptive cruise control on traffic-flow characteristics," *IEEE Trans. Intell. Transp. Syst.*, vol. 7, no. 4, pp. 429–436, Dec. 2006.

[4] S. Shladover, "PATH at 20-History and major milestones," *IEEE Trans. Intell. Transp. Syst.*, vol. 8, no. 4, pp. 584–592, Dec. 2007.

[5] A. Al Alam, A. Gattami, and K. Johansson, "An experimental study on the fuel reduction potential of heavy duty vehicle platooning," in *Proc. IEEE 13th Int. Conf. Intell. Transp. Syst.*, 2010, pp. 306–311.

[6] J. Zhou and H. Peng, "Range policy of adaptive cruise control vehicles for improved flow stability and string stability," *IEEE Trans. Intell. Transp. Syst.*, vol. 6, no. 2, pp. 229–237, Jun. 2005.

[7] G. Naus, R. Vugts, J. Ploeg, M. van De Molengraft, and M. Steinbuch, "String-stable CACC design and experimental validation: A frequency-domain approach," *IEEE Trans. Veh. Technol.*, vol. 59, no. 9, pp. 4268–4279, Nov. 2010.

[8] F. Lin, M. Fardad, and M. Jovanovic, "Optimal control of vehicular formations with nearest neighbor interactions," *IEEE Trans. Autom. Control*, vol. 57, no. 9, pp. 2203–2218, Sep. 2012.

[9] X. Hu, H. Wang, and X. Tang, "Cyber-physical control for energy-saving vehicle following with connectivity," *IEEE Trans. Indus. Electron.*, vol. 64, no. 11, pp. 8578–8587, Nov. 2017.
[10] L. Xiao and F. Gao, "Practical string stability of platoon of adaptive cruise control vehicles," *IEEE Trans. Intell. Transp. Syst.*, vol. 12, no. 4, pp. 1184–1194, Dec. 2011.
[11] J. Ploeg, D. Shukla, N. van de Wouw, and H. Nijmeijer, "Controller synthesis for string stability of vehicle platoons," *IEEE Trans. Intell. Transp. Syst.*, vol. 15, no. 2, pp. 854–865, Apr. 2014.
[12] Y. Zheng, S. E. Li, J. Wang, D. Cao, and K. Li, "Stability and scalability of homogeneous vehicular platoon: Study on the influence of information flow topologies," *IEEE Trans. Intell. Transp. Syst.*, vol. 17, no. 1, pp. 14–26, Jan. 2016.
[13] M. Goli and A. Eskandarian, "Evaluation of lateral trajectories with different controllers for multi-vehicle merging in platoon," in *Proc. IEEE Inter. Conf. Connected Veh. Expo.*, 2014, pp. 673–678.
[14] J. Guo, Y. Luo, and K. Li, "Adaptive fuzzy sliding mode control for coordinated longitudinal and lateral motions of multiple autonomous vehicles in a platoon," *Sci. China Technol. Sci.*, vol. 60, no. 4, pp. 576–586, 2017.
[15] G. Guo and W. Yue, "Autonomous platoon control allowing range-limited sensors," *IEEE Trans. Veh. Technol.*, vol. 61, no. 7, pp. 2901–2912, Sep. 2012.
[16] Y. Zheng, S. E. Li, K. Li, F. Borrelli, and K. Hedrick, "Distributed model predictive control for heterogeneous vehicle platoons under unidirectional topologies," *IEEE Trans. Control Syst. Technol.*, vol. 25, no. 3, pp. 899–910, May 2017.
[17] W. Dunbar and D. Caveney, "Distributed receding horizon control of vehicle platoons: Stability and string stability," *IEEE Trans. Autom. Control*, vol. 57, no. 3, pp. 620–633, Mar. 2012.
[18] S. Oncu, J. Ploeg, N. Van de Wouw, and H. Nijmeijer, "Cooperative adaptive cruise control: Network-aware analysis of string stability," *IEEE Trans. Intell. Transp. Syst.*, vol. 15, no. 4, pp. 1527–1537, Aug. 2014.
[19] B. Besselink and K. Johansson, "String stability and a delay-based spacing policy for vehicle platoons subject to disturbances," *IEEE Trans. Autom. Control*, vol. 62, no. 9, pp. 4376–4391, Sep. 2017.
[20] F. Gao, X. Hu, S. E. Li, K. Li, and Q. Sun, "Distributed adaptive sliding mode control of vehicular platoon with uncertain interaction topology," *IEEE Trans. Indus. Electron.*, vol. 65, no. 8, pp. 6352–6361, Aug. 2018.
[21] X. Guo, J. Wang, F. Liao, and R. S. Teo, "Distributed adaptive integrated-sliding-mode controller synthesis for string stability of vehicle platoons," *IEEE Trans. Intell. Transp. Syst.*, vol. 17, no. 9, pp. 2419–2429, Sep. 2016.
[22] G. Guo and W. Yue, "Hierarchical platoon control with heterogeneous information feedback," *IET Control Theory Appl.*, vol. 5, no. 15, pp. 1766–1781, 2011.
[23] G. Guo and W. Yue, "Autonomous platoon control allowing range-limited sensors," *IEEE Trans. Veh. Technol.*, vol. 61, no. 7, pp. 2901–2912, Sep. 2012.
[24] P. Liu, A. Kurt, and U. Ozguner, "Distributed model predictive control for cooperative and flexible vehicle platooning," *IEEE Trans. Control Syst. Technol*, vol. 27, no. 3, pp. 1115–1128, May 2019.
[25] H. Min, Y. Yang, Y. Fang, P. Sun, and X. Zhao, "Constrained optimization and distributed model predictive control-based merging strategies for adjacent connected autonomous vehicle platoons," *IEEE Access*, vol. 7, pp. 163 085–163 096, 2019.
[26] D. Mayne, M. Seron, and S. Rakovic, "Robust model predictive control of constrained linear systems with bounded disturbances," *Automatica*, vol. 41, no. 2, pp. 219–224, 2005.
[27] D. Mayne and W. Langson, "Robustifying model predictive control of constrained linear systems," *Electron. Lett.*, vol. 37, no. 23, pp. 1422–1423, 2001.
[28] D. Mayne, E. Kerrigan, E. Van Wyk, and P. Falugi, "Tube-based robust nonlinear model predictive control," *Int. J. Robust Nonlinear Control*, vol. 21, no. 11, pp. 1341–1353, 2011.
[29] E. Kayacan, E. Kayacan, H. Ramon, and W. Saeys, "Robust tube-based decentralized nonlinear model predictive control of an autonomous tractor-trailer system," *IEEE/ASME Trans. Mechatron.*, vol. 20, no. 1, pp. 447–456, Feb. 2015.
[30] Y. Gao, A. Gray, E. Tseng, and F. Borrelli, "A tube-based robust nonlinear predictive control approach to semiautonomous ground vehicles," *Veh. Syst. Dyn.*, vol. 52, no. 6, pp. 802–823, 2014.
[31] E. C. Kerrigan, "Robust constraint satisfaction: Invariant sets and predictive control," Ph.D. dissertation, Univ. of Cambridge, 2001.
[32] S. Rakovic, E. Kerrigan, K. Kouramas, and D. Mayne, "Invariant approximations of robustly positively invariant sets for constrained linear discrete-time systems subject to bounded disturbances," Univ. of Cambridge, 2004.
[33] S. Rakovic, E. Kerrigan, K. Kouramas, and D. Mayne, "Invariant approximations of the minimal robust positively invariant set," *IEEE Trans. Autom. Control*, vol. 50, no. 3, pp. 406–410, Mar. 2005.
[34] H. Sira-Ramirez and M. A. Oliver-Salazar, "On the robust control of buck-converter dc-motor combinations," *IEEE Trans. Power Electron.*, vol. 28, no. 8, pp. 3912–3922, Aug. 2013.
[35] B. R. Barmish and G. Leitmann, "On ultimate boundedness control of uncertain systems in the absence of matching condition," *IEEE Trans. Autom. Control*, vol. 27, no. 1, pp. 153–158, Feb. 1982.
[36] G. Rdnyi, "An adaptive spacing policy guaranteeing string stability in multi-brand ad hoc platoons," *IEEE Trans. Intell. Transp. Syst.*, vol. 19, no. 6, pp. 1902–1912, Jun. 2018.
[37] Y. Li, C. Tang, S. Peeta, and Y. Wang, "Nonlinear consensus-based connected vehicle platoon control incorporating car-following interactions and heterogeneous time delays," *IEEE Trans. Intell. Transp. Syst.*, vol. 20, no. 6, pp. 2209–2219, Jun. 2019.
[38] W.-H. Chen, J. Yang, L. Guo, and S. Li, "Disturbance-observer-based control and related methods: An overview," *IEEE Trans. Indus. Electron.*, vol. 63, no. 2, pp. 1083–1095, Feb. 2016.
[39] Y. Wang and S. Boyd, "Fast model predictive control using online optimization," *IEEE Trans. Control Syst. Technol.*, vol. 18, no. 2, pp. 267–278, Mar. 2010.
[40] C. de Souza and L. Xie, "On the discrete-time bounded real lemma with application in the characterization of static state feedback $\mathscr{H}_\infty$ controllers," *Syst. Control Lett.*, vol. 18, no. 1, pp. 61–71, 1992.
[41] R. Eberhart and Y. Shi, "Comparison between genetic algorithms and particle swarm optimization," in *Proc. Int. Conf. Evolut. Prog.*, 1998, pp. 611–616.
[42] K. Kouramas, "Control of linear systems with state and control constraints," Ph.D. dissertation, Univ. of London, 2002.
[43] M. Kvasnica, P. Grieder, M. Baotic, and M. Morari, "Multi-parametric toolbox (mpt)," in *Proc. Int. Workshop Hybrid Syst.: Comput. Control.*, 2004, pp. 448–462.

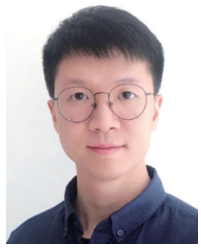

Qianyue Luo received the B.Sc. degree in automotive engineering from the Wuhan University of Technology, Wuhan, China, in 2018. He is currently working toward the M.Sc. degree in automotive engineering from Beihang University, Beijing, China. His research interests include vehicle dynamics and control, multiagent system, and model predictive control.

Anh-Tu Nguyen (Member, IEEE) received the degree in engineering, the M.Sc. degree in automatic control from the Grenoble Institute of Technology, Grenoble, France, in 2009, and the Ph.D. degree in automatic control from the Université Polytechnique Hauts-de-France, Valenciennes, France, in 2013. He is currently an Associate Professor with the INSA Hauts-de-France, Université Polytechnique des Hauts-de-France. After working a short period in 2010 with the French Institute of Petroleum, Rueil-Malmaison, France, He began the doctoral program with the University of Valenciennes, in collaboration with the VALEO Group. From February 2014 to August 2018, he was a Postdoctoral Researcher with the laboratory LAMIH UMR CNRS 8201, Valenciennes, France, and the laboratory LS2N UMR CNRS 6004, Nantes, France. His research interests include robust control, constrained control systems, human-machine shared control for intelligent vehicles.

James Fleming was born in County Durham, U.K., in 1990. He received the M.Eng. and D.Phil. degrees in engineering science from the University of Oxford, Oxford, U.K., in 2012 and 2016, respectively. From 2016 to 2019, he was a Research Fellow within the Faculty of Engineering and Physical Sciences, the University of Southampton, Southampton, U.K.

Since September 2019, he has been a Lecturer with the Wolfson School of Electrical, Mechanical, and Manufacturing Engineering, Loughborough University, Loughborough, U.K. His research interests include the theory and practice of optimal and model predictive control, including applications to fuel-efficient driving, motorcycle stabilization, and wind turbine load mitigation.

Hui Zhang (Senior Member, IEEE) received the B.Sc. degree in mechanical design manufacturing and automation from the Harbin Institute of Technology, Weihai, China, in 2006, the M.Sc. degree in automotive engineering from Jilin University, Changchun, China, in 2008, and the Ph.D. degree in mechanical engineering from the University of Victoria, Victoria, BC, Canada, in 2012.

He was the recipient of the 2017 IEEE Transactions on Fuzzy Systems Outstanding Paper Award, the 2018 SAE Ralph R. Teetor Educational Award, the IEEE Vehicular Technology Society 2019 Best Vehicular Electronics Paper Award, and the 2019 SAE International Intelligent and Connected Vehicles Symposium Best Paper Award. He is a Member of SAE International and ASME. He was an Associate Editor for the IEEE TRANSACTIONS ON VEHICULAR TECHNOLOGY, the IEEE OPEN JOURNAL OF THE INDUSTRIAL ELECTRONICS SOCIETY, *The Journal of the Franklin Institute*, the *SAE International Journal of Connected and Automated Vehicles*, and the *ASME Transactions Journal of Dynamic Systems, Measurement and Control*, and a Board Member of the *International Journal of Hybrid and Electric Vehicles* and the *Mechanical Systems and Signal Processing*.